Novel design of high resolution parallax-free Compton enhanced PET scanner dedicated to brain research

A. BRAEM[1], M. CHAMIZO LLATAS[4], E. CHESI[1], J.G. CORREIA[6], F. GARIBALDI [2], C. JORAM[1], S. MATHOT[1], E. NAPPI[3], M. RIBEIRO DA SILVA[6], F. SCHOENAHL[5], J. SÉGUINOT[1], P. WEILHAMMER[1] and H. ZAIDI[5†]

[1]CERN, EP Division, CH-1211 Geneva, Switzerland
[2]Istituto Superiore di Sanita, Roma, Italy
[3]INFN, Sezione di Bari, Bari, Italy
[4]Geneva University, Dept. of Corpuscular and Nuclear Physics, Geneva, Switzerland
[5]Division of Nuclear Medicine, Geneva University Hospital, CH-1211 Geneva, Switzerland
[6]Instituto Tecnologico e Nuclear, Sacavém, Portugal

Tel: +41 22 372 7258
Fax: +41 22 372 7169
email: habib.zaidi@hcuge.ch

Summary

A novel concept for a Positron Emission Tomography (PET) camera module is proposed, which provides full 3D reconstruction with high resolution over the total detector volume, free of parallax errors. The key components are a matrix of long scintillator crystals and Hybrid Photon Detectors (HPDs) with matched segmentation and integrated readout electronics. The HPDs read out the two ends of the scintillator package. Both excellent spatial (*x*,*y*,*z*) and energy resolution is obtained. The concept allows enhancing the detection efficiency by reconstructing a significant fraction of events which underwent Compton scattering in the crystals. The proof of concept will first be demonstrated with yttrium orthoaluminate perovskite (YAP):Ce but the final design will rely on other scintillators more adequate for PET applications (e.g. LSO:Ce or $LaBr_3$:Ce). A promising application of the proposed camera module, which is currently under study, is a high resolution 3D brain PET camera with an axial field-of-view of ~10-15 cm dedicated to brain research. The design philosophy, software development aspects and other potential applications like PE mammography (PEM) are also discussed.

Key words. Positron emission tomography, functional brain imaging, hybrid photon detectors, Compton enhancement, simulation.

Short running title: Novel design of a PET scanner dedicated to brain research

† Corresponding author, e-mail: habib.zaidi@hcuge.ch

1. Introduction

Positron Emission Tomography (PET) provides qualitative as well as quantitative information about the volume distribution of biologically significant radiotracers after injection into the human body. Unlike X-ray computed tomography (CT) or magnetic resonance imaging (MRI), which look at anatomy or body morphology, PET studies metabolic activity and tissue function. Within the spectrum of medical imaging modalities, sensitivity ranges from the detection of milli-molar concentrations in functional MRI to pico-molar concentrations in PET, which gives a 10^9 difference (Phelps, 2000). With respect to specificity, the range is from detecting tissue density and water content to a clearly identified molecule labelled with a radioactive form of one of its natural constitutive elements. This sensitivity is a prerequisite if studies are to be undertaken of pathways and binding sites which function at less than the micro-molar level, and to avoid the pharmacological effects of administering a labelled molecule to study its inherent bio-distribution.

Advances in quantification of brain function (blood flow, metabolism and receptor characteristics) with PET, especially for small structures, rely on two aspects: (i) improvements in instrumentation to enhance spatial resolution and sensitivity, and development of components to correct for physical degrading factors; and (ii) improvements in algorithmic design to attain better image quality and achieve more accurate and automated quantification of physiological parameters. The challenge for advanced PET instrumentation is the optimisation of the performance in terms of spatial resolution, contrast and sensitivity, at minimized fabrication and operation cost of the PET scanner (Phelps and Cherry, 1998). As PET has become of more interest for clinical practice, several different design trends seem to have developed (Phelps, 2000). Systems are being designed for "low cost" clinical applications, very high resolution research applications, and just about everywhere in-between. All of these systems are undergoing revisions in both hardware and software components.

New detector technologies that are emerging include the use of new scintillating materials as detectors including new Cerium-doped, fast and high effective-Z crystals like gadolinium orthosilicate (GSO:Ce), lutetium oxyorthosilicate (LSO:Ce), lutetium orthoaluminate perovskite (LuAP:Ce) and Lanthanum Halide scintillators ($LaBr_3$:Ce) as alternatives to bismuth germanate (BGO) crystals, the use of layered crystals and other schemes for depth-of-interaction determination (van Eijk, 2002). In addition, high resolution animal scanner designs are plentiful and many such devices are now being offered commercially. The most important

aspect related to the outcome of research performed in the field is the improvement of the cost/performance optimisation of clinical PET systems.

Significant progress has been made by different scanner manufacturers and research groups in the design of high resolution 3D PET units with the capacity to acquire more accurate depth-of-interaction (DOI) information to reduce the parallax error. However, emerging clinical and research applications of brain imaging demand even greater levels of accuracy and precision and therefore impose more constraints on hardware and software aspects, especially with respect to the intrinsic performance of the PET tomograph. Continuous efforts to integrate recent research findings for the design of PET scanners have become the goal of both the academic community and nuclear medicine industry. In this perspective, we propose a novel and innovative 3D brain PET concept[1], which is complementary to existing commercial (Wienhard et al., 2002) and prototype PET scanners currently under development (Surti et al., 2001, Watanabe et al., 2002). This concept leads to an image reconstruction which is free of any parallax error and provides a uniform spatial and energy resolution over the whole sensitive volume. Furthermore it allows enhancing the sensitivity by reconstructing a substantial fraction of events which underwent Compton scattering in the detectors. This paper describes the principles of this new concept and the design philosophy as well as the basic components if the PET camera modules under development within the framework of the Computer Imaging for Medical Applications (CIMA) collaboration[2] hosted by CERN.

2. Motivations for a high resolution PET scanner dedicated to functional brain imaging

Current dedicated PET scanners employ conventional detector blocks consisting of several stacked rings of inorganic scintillating crystals radially oriented and readout on the backside by standard photomultiplier tubes (PMTs) or multi-anode PMTs. The depth of interaction of the detected photons in the crystal is not measurable in such a configuration and gives rise to intrinsic parallax errors, hence an image degradation depending on the emission point in the transaxial plane. This inherent limitation is coped with by keeping the radial length of the crystal small, typically on values around the attenuation length at 511 keV, which however strongly compromises the detection efficiency. The phoswich approach, which leads to a better approximation of the interaction point, has recently been implemented in the ECAT high resolution research tomograph (HRRT) (Wienhard et al., 2002), which we consider as the current reference in brain PET technology (Watanabe et al., 2002, Surti et al., 2001). The

[1] patent applied for PCT/EP 02/07967
[2] http://www.cima-collaboration.org/

HRRT has a field-of-view (FOV) of 25.2 cm axially and 31.2 cm transaxially. It achieves a spatial resolution (FWHM) of 2.4 mm at the center of the FOV and 2.8 mm at 10 cm of center transaxially and 2.6 to 5 mm axially depending on axial compression mode and reconstruction procedure. The energy resolution varies between 14-18% (Schmand et al., 1998). A sensitivity of 4.5 cps/kBq (trues+scatter) and a maximum noise equivalent count (NEC) rate of 230 kcps reached at 37 kBq/ml have been measured with a cylinder of 20 cm diameter and 20 cm length filled with ^{18}F dissolved in water. The intrinsic physical performance of conventional designs seem to have been reached encouraging the development of innovative approaches capable of providing improved performance at a reduced or comparable cost.

3. The HPD-PET concept

Over the last years, the European Organization for Nuclear Research (CERN) has developed the facilities to develop and build Hybrid Photon Detectors (HPDs) including designs with a proximity focused optics and thin sapphire entrance windows. Its infrastructure and well developed links to numerous institutions, naturally grown over decades in international scientific collaborations, let CERN appear as ideal technical leader in projects related to the design of medical imaging systems. The proposed innovative HPD 3D axial detector concept is based on recent substantial development efforts in high energy physics instrumentation, undertaken at CERN in collaboration with other research institutes, universities and companies. A key component is the large area highly pixelized HPD with its integrated self triggering readout electronics (Joram, 1999, Weilhammer, 2000, Braem et al., 2003). The particular features of this photodetector technology allow for a cost efficient readout of finely segmented arrays of scintillator crystals.

Our 3D brain PET concept overcomes the parallax problem by means of a novel geometric configuration. The proposed 3D PET camera module consists of an array of long (100 to 150 mm) crystals of small cross-section (e.g. 3.2×3.2 mm^2). This axially oriented array of crystals (e.g. 13 ×16) is read out on both sides by HPDs. Fig. 1 shows the principle of the 3D HPD-based Compton-enhanced PET design. The size and segmentation of the Silicon sensor matches exactly with the crystal matrix. This highly segmented geometry provides an accurate and uniform resolution in the transaxial (*x*-*y*) plane of 1.7 to 1.9 mm (FWHM), completely independent of the radial detector thickness. The latter can therefore be increased to 2-3 attenuation lengths, which essentially doubles the sensitivity compared to conventional block detector approach. The transaxial segmentation allows tracking multiple interactions of annihilation photons in the scintillator matrix, which provides the possibility to reconstruct a

large fraction of Compton scattered events. This results in a further sensitivity increase by a factor 2-3. The axial coordinate (z) is derived with good precision from the asymmetry of the light intensity detected at the two ends of the scintillating crystals. Hence, the coincident event is reconstructed in fully 3D mode without any parallax effects irrespective of the annihilation point. This is expected to lead to a spatial and energy resolution, which is superior to any known comparable system and completely uniform over the whole detection volume. A remarkable improvement in image quality and quantitative accuracy could consequently be attained. The achievable spatial (z) and energy resolution as well as the sensitivity depend on the choice of the scintillation crystal and will be discussed below.

4. Design considerations

The steps required to build the PET camera modules with the specifications claimed above comprise several distinct major components or work blocks, for which a well defined sharing of responsibilities amongst the participating institutes has been defined. In the following we describe the hardware components to be developed, characterized and validated.

4.1. Fast inorganic scintillation crystals

The choice of the scintillator is a fundamental element of a PET design. The project will profit from recent progress in the development and growing of crystals with optimised characteristics and the associated machining (cutting and polishing) techniques. On the medium term Cerium doped Lutetium orthosilicate (LSO:Ce), produced by CTI PET Systems (Knoxville, TN) and Cerium doped Lanthanum Bromide ($LaBr_3$:Ce), under development by Saint Gobain (France), are the most promising candidates. They combine high density and high atomic number necessary for an efficient photoelectric conversion of the annihilation photons, with a short decay time of the scintillation light, which is a key requirement for high counting rates. Table 1 summarizes these properties for selected scintillators currently in use and under development for PET applications. The final choice will be made after an in-depth investigation of the physical characteristics including light yield, energy resolution, linearity of response with energy, light absorption coefficient at wavelength of emission, mechanical properties and surface quality of long crystal bars, availability and cost.

An advantage of LSO compared to $LaBr_3$ is its high photoelectric cross section, but it is substantially worse in terms of energy resolution and response linearity. Also the decay time of LSO is longer than the one of $LaBr_3$. However, this crystal is still in a development phase at Saint Gobain and not yet commercially available. It is worth emphasizing that a recent study reported that the combination of excellent energy resolution and timing resolution of $LaBr_3$

can potentially lead to a very significant improvement in PET performance (Surti et al., 2003). To avoid unnecessary delays, the collaboration decided to initially demonstrate the innovative features of the HPD-PET concept and explore its potential with YAP:Ce crystals, although its physical characteristics are not optimal. Though, the material is inexpensive, commercially available and can be machined and polished to long bars.

For the 3D axial detector geometry 208 (13 x 16) long crystals of 3.2 x 3.2 mm^2 cross section are arranged to a matrix with gaps of 0.8 mm between crystals. Scintillation light produced after an interaction of an annihilation photon, propagates by total internal reflection to the ends, where it is detected by the HPD photodetectors.

The high light output of the YAP:Ce crystal bars, combined with the excellent pulse height resolution of the HPD, results in a system energy resolution of ~7-7.5% (FWHM), which is significantly better than resolutions quoted for existing systems. The spatial resolution in the axial coordinate is expected to be 4.5 mm (FWHM). Both the z- and energy resolution would significantly improve if $LaBr_3$ crystals become available. Detailed calculation for a brain PET scanner with 35 cm free inner diameter and 10 cm axial FOV (Fig. 2), based on the proposed axial approach and equipped with LSO:Ce or LaBr3:Ce crystals, let expect a sensitivity of 3-4 cps/kBq and a NEC of about 130 kcps (under the conditions described above for the HRRT scanner). This value is comparable to the HRRT scanner, one of the most advanced systems, which has however an axial FOV of 25 cm (compared to 10 cm in our design).

4.2. Hybrid Photon Detectors

The photodetectors, which are coupled to both ends of the crystal array, are proximity focused HPDs with a thin (1.8 mm) flat sapphire entrance window. Keeping this window as thin as possible minimizes the widening of the light cone when it propagates from the scintillation crystal to the photocathode of the HPD deposited on the inner surface of the window. The quantum efficiency of the photocathode is about 25% at the wavelength of maximum emission of $LaBr_3$ and 18% for LSO. The proximity focusing electron optics of the HPD produces a 1:1 image of the scintillator array onto the Silicon sensor, which is segmented into 208 (13 x 16) diode pads of 4×4 mm^2 size, precisely matching the pattern of the crystal array. The sensor is mounted on a ceramic carrier which receives the two front-end chips (type VATA, 128 channels/chip). Wire bonds link the chips to the sensor. The HPDs are operated at a moderate cathode potential of about 12 kV, sufficient for a signal of about 3000 electron-hole pairs in the Silicon sensor for every detected photoelectron.

While in the initial phase of the project a round HPD with ceramic body will be used to assemble a PET camera module for the proof of principle, the early demonstrator requires a

rectangular HPD with optimised geometry to increase the inner free diameter of the scanner and improve the azimuthal coverage. During the last years the CERN group has built numerous HPDs with a diameter of 127 mm and 16 readout chips (2048 channels) encapsulated inside the vacuum envelope. The complex technical facilities for the preparation of components and the photocathode processing and encapsulation of round HPDs are available. A moderate upgrade of the facilities will allow fabricating also rectangular devices.

4.3. Front-end electronics

The front-end electronics, which amplifies, shapes, samples and temporarily stores the signal produced in the Silicon sensor of the HPD is another key component of the concept. We plan to use a fast version of the VLSI chip VATA-GP3, developed by IDEAS in collaboration with CERN. The existing version of this chip has 128 channels and provides a self triggering operation mode, as required for PET, and a so-called sparse readout option, i.e. only hit channels are read out. The excellent performance of this chip has recently been demonstrated (Chesi and al., 2003). Each electronic channel comprises:

- a 'slow' analog chain with a charge sensitive amplifier, and a shaper of 3 μs time constant for low-noise pulse height determination. The sampled maximum pulse height is stored in a register for later readout
- a 'fast' chain with additional amplification, fast shaping (150 ns) and discrimination. It is the logical 'OR' of all 128 discriminators which is interpreted as trigger signal for the readout of the pulse height information.

In contrast to a conventional serial readout mode, where after a trigger all 128 channels would be readout, in sparse mode only those channels with a discriminated hit obtain a readout tag. This feature strongly shortens the overall readout time, particularly if typically only one or very few channels are hit. The current version already comprises numerous features which are indispensable for a PET system like blocking and reset mechanisms, masking, fine adjustment of thresholds and calibration. For a full demonstration of its performance in PET operation, the chip design needs to undergo further development iterations:

- The dynamic range of the input stage is adapted from currently 18 fC to about 400 fC to handle the typical charge level in the Silicon detector during PET operation.
- To achieve shaping time constants of 25 and 150 ns, respectively, required for PET coincidence timing in a 5 ns interval and high rate operation, the chip needs to be implemented in deep sub-micron technology (e.g. 0.35 μm CMOS). In addition time walk

compensation (or constant fraction discrimination), minimized propagation times of control signals and 20 MHz readout clock speed need to be implemented.

4.4. HPD 3D axial camera module

A HPD 3D axial camera module consists of a matrix assembly of 208 (13 x 16) long scintillation crystals, optically coupled to a pair of HPD photodetectors. We foresee to fabricate a first camera module, called 'module A', using round HPDs (PCR5) and a matrix of 64 YAP:Ce crystals. At a later stage, we intend to demonstrate the full performance of the HPD-PET concept in an arrangement of four final camera modules, called 'module B', employing optimized rectangular HPDs, fast electronics, final scintillation crystals and the PET data acquisition system discussed in the following section.

4.5. Data acquisition system

The data acquisition system of a PET camera needs to cope with high single and coincidence count rates as well as high data taking rates. Our approach, tailored to the specific characteristics of the HPD front-end electronics, consists of parallel fast coincidence processors coupled to high density storage media and one asynchronous readout chain for each camera module.

A 'good' PET event is defined as the time-coincident detection of two annihilation quanta of 511 keV energy emitted in a back-to-back configuration. Coincidences are formed on the level of camera modules. The counting rate of each module under the test conditions of the NEMA-NU2 protocol with a cylindrical phantom (20 cm diameter and 20 cm length) of 13 kBq/ml activity (total activity = 81.4 MBq) are of the order 1.5 MHz. To limit the rate of accidental coincidences between modules, the coincidence time window has to be kept at values ≤5 ns. Reading out the information stored in the 4 front-end chips of a module leads to a dead time fraction of less than 10%. The concept of parallel coincidence processors permits to initiate the readout sequence only for those two modules which form a coincidence, while all other modules stay active, thus minimising the system dead-time. We expect the parallel readout chains to record the (trues+scatter) data of each module at a rate of about 200 kHz. The raw data will be stored on fast hard disks of at least 100 Gb storage capacity.

5. Software aspects

On the software side, we aim to develop the required software packages to simulate design aspects of the prototype, correct the data for physical degrading effects and reconstruct images

from measured data as well as the graphical user interface and image display and analysis utilities required to validate and exploit the system in a clinical and research environment.

5.1. Monte Carlo simulation of the HPD-PET design

Monte Carlo simulation techniques constitute the gold standard and were extensively used to analyze the performance of new potential designs of nuclear medicine imaging systems including PET. There exist several Monte Carlo simulation packages that run under any standard operating system environments and are easily extendible to new scanners' geometrical configurations. The software package that will be used in this work is based on a modified version of a PET simulator based on GEANT platform (Agostinelli, 2002) developed at CERN for high energy physics experiments, developed mainly for the cylindrical multi-ring geometry (Zaidi et al., 1999). We anticipated that the possibilities offered by the software need to increase steadily according to the research application of interest. Therefore software changes would be unavoidable within the following years. Besides extendibility, maintainability was thus very important as existing code must be reused and new features must be introduced in a straightforward manner. The object-oriented programming paradigm meets all these requirements and has proven to improve productivity, quality, and innovation in software development. It provides modelling primitives, a framework for high-level reusability, and integrating mechanisms for organizing knowledge about application domains. The package is structured to be a convenient test bench to develop software modules that can be integrated into conventional C/C++ programs. We aim to further develop and exploit this package to optimize the design of the HPD-PET scanner. Segmentation will be added step by step to the software and detailed modules descriptions to produce specifications for the final design.

5.2. Image reconstruction and correction for physical degrading factors

Two major classes of image reconstruction algorithms are used in PET: direct analytical methods and iterative methods. An undesirable property of the iterative Maximum Likelihood Expectation-Maximization (ML-EM) algorithm is that large numbers of iterations increase the noise content of the reconstructed images. These noise characteristics can be controlled in iterative algorithms that incorporate a prior distribution to describe the statistical properties of the unknown image and thus produce *a posteriori* probability distributions from the image conditioned upon the data. Bayesian reconstruction methods form a powerful extension of the ML-EM algorithm. Maximization of the *a posteriori* (MAP) probability over the set of possible images results in the MAP estimate. From the developer's point of view, a significant

advantage of this approach is its modularity: the various components of the prior, such as non-negativity of the solution, pseudo-Poisson nature of statistics, local voxel correlations (local smoothness), or known existence of anatomical boundaries, may be added one by one into the estimation process, assessed individually, and used to guarantee a fast working implementation of preliminary versions of the algorithms. The reconstruction package will be based on an updated version of the STIR open source reconstruction library[3] to reconstruct images from data acquired in list-mode format.

To obtain quantitative data in PET it is necessary to estimate and subtract major physical phenomena that degrade the data sets. The non-homogeneous distribution of attenuation coefficients due to presence of air cavities and sinuses complicates the interpretation of 3D brain PET images and precludes the application of simple methods of scatter and attenuation correction developed for homogeneous media. Moreover, the problem of scatter correction is of paramount importance in high resolution PET imaging in which the scatter degradation features become more complex. Therefore, we will focus on correction schemes for resolution recovery, and attenuation and scatter corrections applied either before or integrated in the reconstruction process. Models for accurate quantitative analysis using combined MRI and PET data developed at Geneva University Hospital will also be further developed and used on this transmissionless device (Zaidi et al., 2003).

6. Conclusions and future work

The limitations of current PET instrumentation dedicated to brain imaging motivates the development of new technologies capable of responding to current needs of clinical and research neuroscience investigators. We have described a novel concept for the design of a PET camera module dedicated for brain research, which provides full 3D reconstruction with high resolution over the total detector volume, free of parallax errors. The CIMA collaboration at CERN is actively engaged in the design of this new device, which, if successful, will be used to obtain new information on brain diseases and understand functionalities of the human brain. The concept seems also to be promising for positron emission mammography (PEM) where both high spatial resolution and sensitivity are required to meet the needs of early detection of breast tumours hence avoiding biopsy intervention.

Acknowledgements

We would like to thank J.M. LeGoff and R. Amendolia (CERN ETT-TT) for the continuous support of this project. The construction of the prototype HPDs would not have been possible

[3] http://stir.irsl.org/

without the competent work of numerous technical collaborators, particularly C. David and I. Mcgill (CERN EP-TA1). This work was supported in part by the Swiss National Science Foundation under grant SNSF 3152A0-102143.

References

Agostinelli, S. e. a., "Geant4 - a simulation toolkit." *Technical Report CERN-IT-20020003* (CERN European Laboratory for Particle Physics, Geneva, Switzerland, 2002, Geneva, 2002).

Braem, A., Chesi, E., Hammarstedt, P., et al. (2003) The Pad HPD: A highly segmented hybrid photodiode. *Nucl Instr Meth A* **497:** 202-205.

Chesi, E. and al., e. (2003) The VATAGP3 test set-up and first results from measurements with the VATAGP3 chip. *Nucl Instr Meth A submitted*

Joram, C. (1999) Large area hybrid photodiodes. *Nucl Phys B* **78:** 407-415.

Phelps, M. E. (2000) PET: the merging of biology and imaging into molecular imaging. *J Nucl Med* **41:** 661-681.

Phelps, M. E. and Cherry, S. R. (1998) The changing design of positron imaging systems. *Clin. Pos. Imag.* **1:** 31-45.

Schmand, M., Eriksson, L., Casey, M. E., et al. (1998) Performance results of a new DOI detector block for a high resolution PET-LSO research tomograph HRRT. *IEEE Trans Nucl Sci* **45:** 3000-3006.

Surti, S., Karp, J., Muehllehner, G., et al. (2003) Investigation of Lanthanum scintillators for 3-D PET. *IEEE Trans Nucl Sci* **50:** 348-354.

Surti, S., Karp, J. S., Adam, L.-E., et al. (2001) "Performance measurements for the GSO-based brain PET camera (G-PET).," In *Proc.* IEEE Nuclear Science Symposium and Medical Imaging Conference., Oct. 4-10, San Diego, CA, pp. 1109-1114.

van Eijk, C. W. E. (2002) Inorganic scintillators in medical imaging. *Phys Med Biol* **47:** R85-R106.

Watanabe, M., Shimizu, K., Omura, T., et al. (2002) A new high-resolution PET scanner dedicated to brain research. *IEEE Trans Nucl Sci* **49:** 634-639.

Weilhammer, P. (2000) Silicon-based HPD development: sensors and front ends. *Nucl Instr Meth A* **446:** 289-298.

Wienhard, K., Schmand, M., Casey, M. E., et al. (2002) The ECAT HRRT: performance and first clinical application of the new high resolution research tomograph. *IEEE Trans Nucl Sci* **49:** 104 -110.

Chesi, E., et al. (2003) The VATAGP3 Test Set-up and First Results from Measurements with the VATAGP3 Chip, in preparation for publication in Nucl. Instr. Meth. A.Zaidi, H., Herrmann Scheurer, A. and Morel, C. (1999) An object-oriented Monte Carlo simulator for 3D positron tomographs. *Comput Meth Prog Biomed* **58:** 133-145.

Zaidi, H., Montandon, M.-L. and Slosman, D. O. (2003) Magnetic resonance imaging-guided attenuation and scatter corrections in three-dimensional brain positron emission tomography. *Med Phys* **30:** 937-948.

Figure legends

Fig. 1. Principle of HPD-based 3D Compton-enhanced PET camera module.

Fig. 2. Illustration of principles of data acquisition for a brain PET camera using the conventional cylindrical multi-ring geometry based on detector blocks and readout by PMTs (**A**) and the novel design based on 12 camera modules consisting of long scintillation crystals readout on both sides by HPDs (**B**).

Fig. 3. Illustration of a 3D PET camera module. In this prototype configuration two round HPD photodetectors are coupled to the matrix of scintillators.

Fig. 4. Schematic layout of the VATA front-end chip.

Tables

Table 1. Characteristics of scintillator crystals under development and currently used in commercial and prototype PET tomographs design.

Scintillator	BGO	LSO	GSO	LuAP	$LaBr_3$	YAP
Formula	$Bi_4Ge_3O_{12}$	Lu_2SiO_5:Ce	Gd_2SiO_5:Ce	$LuAlO_3$:Ce	$LaBr_3$:Ce	$YAlO_3$:Ce
Density (g/cc)	7.13	7.4	6.71	8.34	5.3	5.37
Light yield (photons/keV)	9	25	8	10	61	21
Effective Z	75	66	60	65	46.9	34
Principal decay time (ns)	300	42	30-60	18	35	25
Peak wavelength (nm)	480	420	440	365	358	370
Index of refraction	2.15	1.82	1.95	1.95	1.88	1.94
Photofraction (%)*	41.5	32.5	25	30.6	15	4.5
Attenuation length (cm)*	1.04	1.15	1.42	1.05	2.13	2.19
Energy resolution (%)*	7.9	88	6.9	10	2.9	3.8
Hygroscopic	No	No	No	No	Yes	No

* At 511 keV

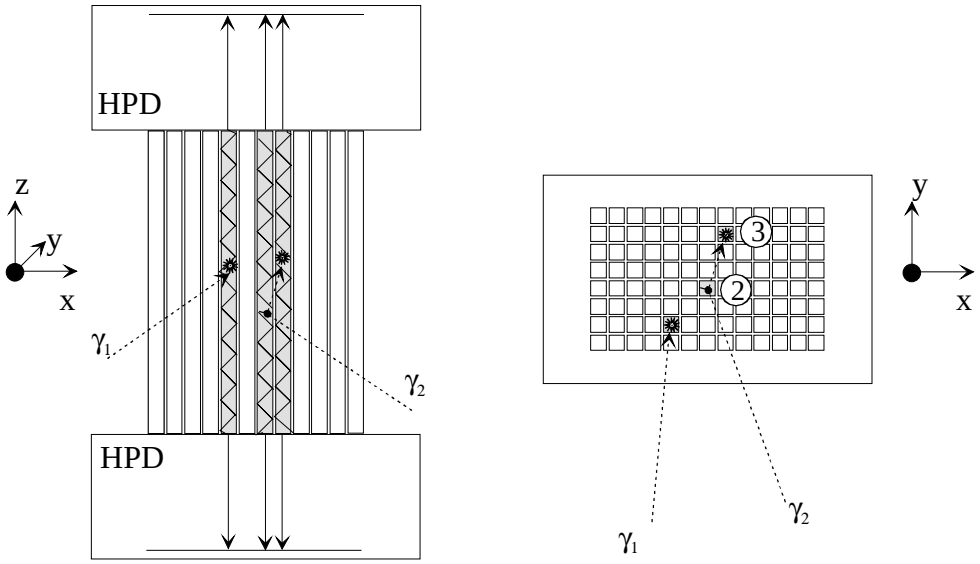

side view sectional view

Fig. 1.

A

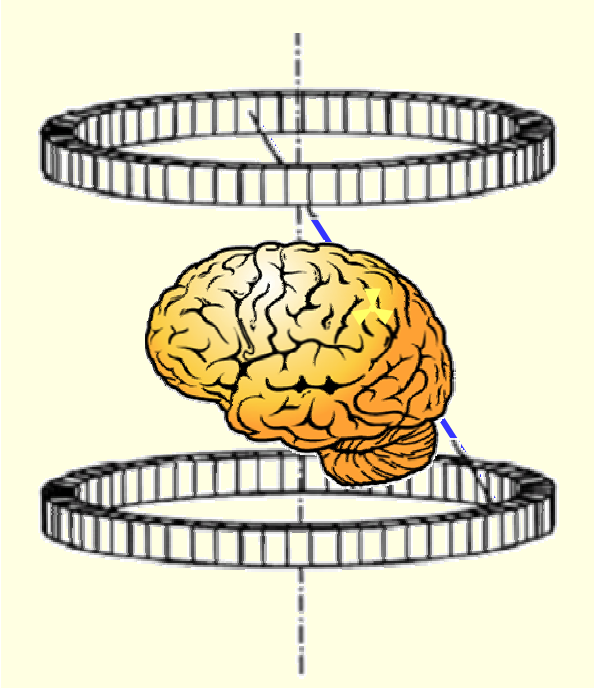

B

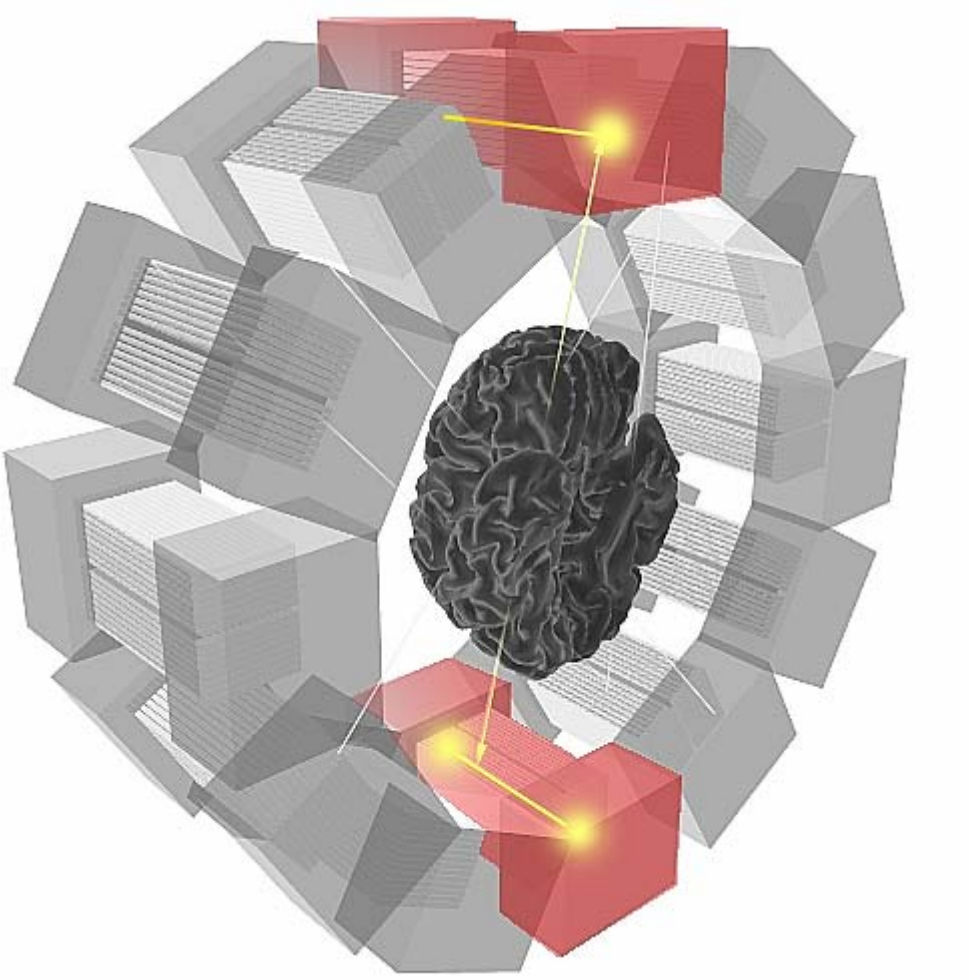

Fig. 2.

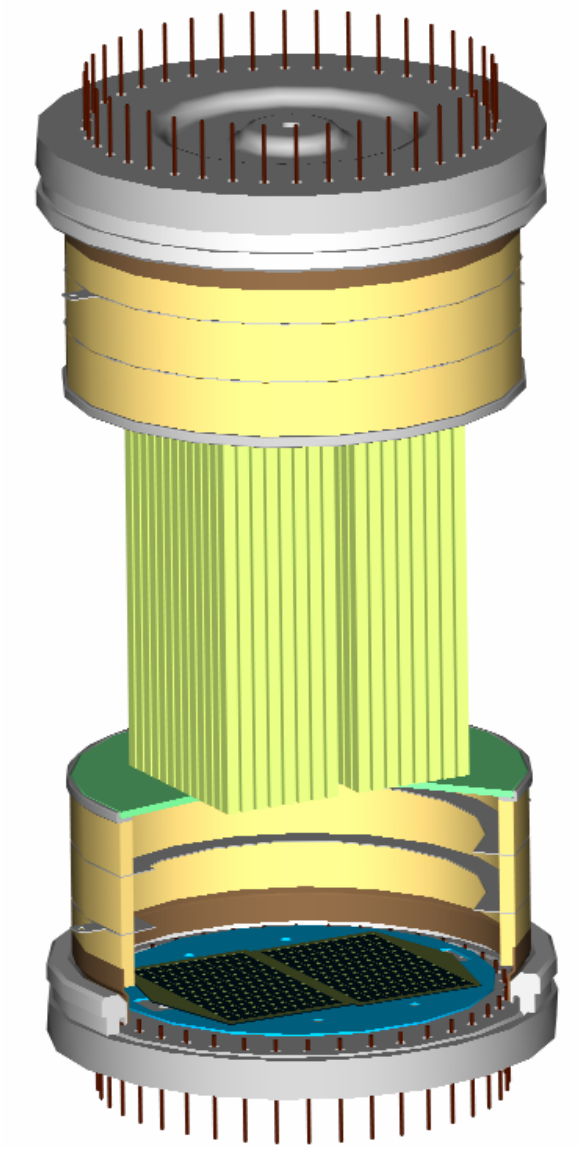

Fig. 3.

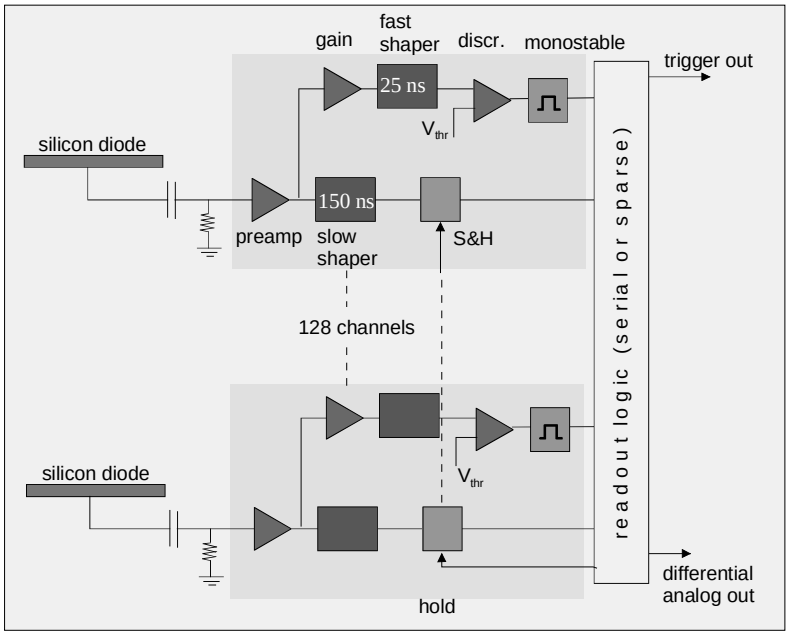
gain
fast shaper
discr.
monostable
trigger out
25 ns
V_{thr}
silicon diode
150 ns
preamp
slow shaper
S&H
128 channels
readout logic (serial or sparse)
silicon diode
V_{thr}
differential analog out
hold

4

Fig. 4.